Vaccine 37 (2019) 5762–5769

Contents lists available at ScienceDirect

Vaccine

journal homepage: www.elsevier.com/locate/vaccine

Assessment of the impact of manufacturing changes on the physicochemical properties of the recombinant vaccine carrier ExoProtein A

Martin Burkhardt [a,1], Karine Reiter [a,1], Vu Nguyen [a], Motoshi Suzuki [b], Raul Herrera [a], Patrick E. Duffy [a], Richard Shimp Jr. [a], Nicholas J. MacDonald [a], L. Renee Olano [b], David L. Narum [a,*]

[a] Laboratory of Malaria Immunology and Vaccinology, National Institute of Allergy and Infectious Diseases, National Institutes of Health, 5640 Fishers Lane, Rockville, MD 20852, United States
[b] Research Technology Branch, National Institute of Allergy and Infectious Diseases, National Institutes of Health, 5640 Fishers Lane, Rockville, MD 20852, United States

ARTICLE INFO

Article history:
Received 4 May 2018
Received in revised form 6 September 2018
Accepted 16 September 2018
Available online 24 September 2018

Keywords:
Vaccine
Vaccine carrier
Malaria
Host cell protein
Mass spectrometry
ExoProtein A
Purification
Mixed-mode chromatography

ABSTRACT

Efforts to develop a vaccine for the elimination of malaria include the use of carrier proteins to assemble monomeric antigens into nanoparticles to maximize immunogenicity. Recombinant ExoProtein A (EPA) is a detoxified form of *Pseudomonas aeruginosa* Exotoxin A which has been used as a carrier in the conjugate vaccine field. A pilot-scale process developed for purification of EPA yielded product that consistently approached a preset upper limit for host cell protein (HCP) content per human dose. To minimize the risk of bulk material exceeding the specification, the purification process was redeveloped using mixed-mode chromatography resins. Purified EPA derived from the primary and redeveloped processes were comparable following full biochemical and biophysical characterization. However, using a process specific immunoassay, the HCP content was shown to decrease from a range of 0.14–0.24% w/w of total protein to below the level of detection with the revised process. The improved process reproducibly yields EPA with highly similar quality characteristics as the original process but with an improved profile for the HCP content.

Published by Elsevier Ltd.

1. Introduction

Effective polysaccharide vaccines have been developed based on a platform of conjugating immunogenic carriers to T-cell independent polysaccharide antigens and the diversity of these carriers has expanded over time. Conjugation of the polyribosylribitol phosphate capsular polysaccharide (PRP) of *Haemophilus influenza* b (Hib) to protein antigen was originally performed using horse immunoglobulin as carrier to successfully increase the intensity and duration of an anti-Hib response [1]. Later, the introduction of tetanus toxoid (TT), CRM197 and protein D as carriers for PRP made possible the production of effective vaccines for the control of Hib related invasive meningococcal disease (IMD) in infants [2–4]. Another carrier includes the outer membrane complexes (OmpC) of *Neisseria meningitides* type b and outer membrane vesicles (OMV) [5]. OMPC and OMV are used in commercially available vaccines for prevention of Hib disease and meningococcal B infections, respectively [6,7].

Conjugates of detoxified *Pseudomonas aeruginosa* recombinant exotoxin A (EPA) developed using knowledge of molecular function have been used in clinical trials and shown to be safe [8–11]. Recombinant EPA differs from the native exotoxin A by a single amino acid deletion (E553) which yields a detoxified form of exotoxin A while maintaining immunogenicity [12]. Although chemical conjugation has been more commonly applied to T-cell independent polysaccharide antigens, protein-protein conjugation was investigated and demonstrated to effectively enhance immunogenicity of a poorly immunogenic recombinant malaria transmission blocking vaccine candidate identified as the *Plasmodium falciparum* 25 kDa sexual stage protein (Pfs25), in both preclinical [13] and clinical studies [11]. These observations have been cooperated using several carriers [14] and has been applied to other recombinant malaria vaccine candidate antigens [15,16]. The protein-protein chemical conjugates have the biophysical appearance of a nanoparticle in solution with a comparable size to that of the virus-like particle from hepatitis B [16,17] used in the leading pre-erythrocytic malaria vaccine RTS,S [18,19]. These

* Corresponding author.
E-mail address: dnarum@niaid.nih.gov (D.L. Narum).
[1] Both authors contributed equally to this work.

https://doi.org/10.1016/j.vaccine.2018.09.037
0264-410X/Published by Elsevier Ltd.

conjugated nanoparticles have excellent quality characteristics for scaled processes [17].

Even though the quality and consistency of the bulk EPA has been acceptable for phase 1 clinical trials [11], during repeated pilot-scale cGMP runs, the *Escherichia coli* (*E. coli*) host cell protein (HCP) content was marginally out of specification and required reprocessing using a single chromatography step selected from the existing process. To correct for these out of specification results, the process [13] was redeveloped with the aim to reduce the HCP content while maintaining the quality and quantity of purified EPA. To this end, two multimodal resins were selected to replace three purification sorbents which improved the reproducibility in removal of HCPs without modifying the quality characteristics already established (Fig. 1). Here, we report the changes in the downstream purification process and the comparability analyses on bulk EPA produced from the original purification process and redeveloped process including the use of mass spectrometry to assess EPA composition and post-translational modifications (PTMs).

2. Materials and methods

2.1. Expression and purification of EPA

The EPA expression in *E. coli* BL21λDE3 strain (Invitrogen) with a kanamycin resistant gene, fermentation conditions using defined media, recovery and purification have been previously reported [13]. The kanamycin expression plasmid pET-24a/rEPA was constructed using the *EPA* gene amplified from pVC45Df+T [20] (also identified as pVC45D [21]). The *EPA* gene was sequenced, and the nucleotide sequence submitted to Genbank (accession number: MH282864). The production process as reported (*i.e.,* process A) [13] was revised (process B) as follows: concentrated and dialyzed fermentation supernatant was diluted 5-fold in Capto Q equilibration buffer (20 mM Bis-Tris, pH 5.9) and loaded onto a Capto Q column (GE Healthcare) at 250 cm/h. The column was washed with 20 mM Bis-Tris, pH 5.9 with 150 mM NaCl for 2 column volumes (CVs) and eluted with the same solution containing 500 mM NaCl.

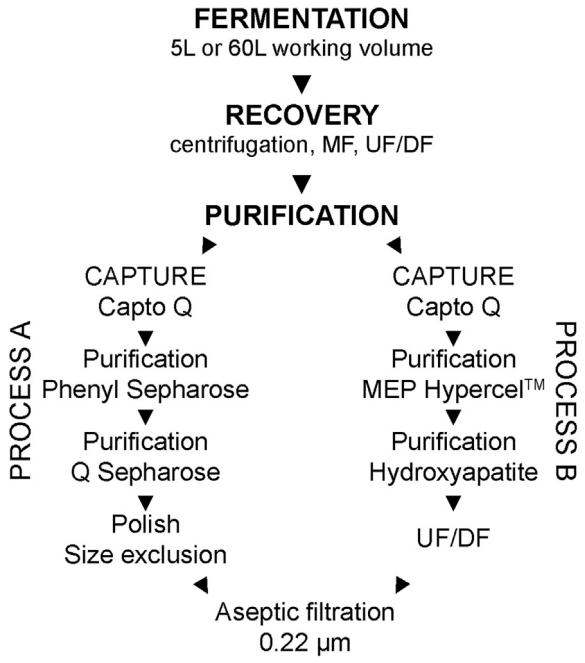

Fig. 1. Process flow diagram for purification of EPA. Process A has been previously reported [13] and the revised process reported here is identified as process B.

For adsorption of EPA on the 4-mercaptoethyl-pyridine (MEP) HyperCel™ sorbent (Pall Corporation), the Capto Q eluent was diluted 1:1 v/v with 100 mM sodium phosphate dibasic heptahydrate with 2 M ammonium sulfate, and 100 mM arginine-HCl (JT Baker), pH 7.8. Equilibration buffer was 500 mM ammonium sulfate, 100 mM sodium phosphate dibasic, 100 mM arginine-HCl, pH 7.8. Unbound material was removed with equilibration buffer at 100 cm/h for 5–6 CVs. The column was then washed with 25 mM acetate with 1.0 M arginine-HCl at pH 5.0 for approximately 8 CVs and EPA was eluted with 100 mM sodium acetate, 1 M arginine-HCl, pH 4.0 at 150 cm/h. The MEP eluent was diluted 10-fold with hydroxyapatite (CHT) equilibration buffer (20 mM sodium phosphate, pH 6.0). The diluted EPA was bound to a CHT type I (Bio-Rad) column in CHT equilibration buffer at 135 cm/h and washed with the same buffer for approximately 5 CVs. EPA was eluted with 10 mM sodium phosphate, pH 7.5. The CHT elution was concentrated and dialyzed with PBS, pH 7.2 to ~3 mg/mL as determined by A_{280} using a 5K NMWC hollow fiber filter (GE Healthcare) and then filtered through a 0.22 μm Millipak-60 filter (Millipore Corp.) and stored at <−70 °C.

2.2. Biochemical and biophysical characterization of EPA

The recombinant EPA proteins were fully characterized using similar techniques to those previously reported [13,17,22]. Protein separation by analytical size exclusion chromatography (SEC)-HPLC was performed on a TSKgel G3000SWxl column (Tosoh Biosciences) with in-line multi-angle light scattering (MALS) (Wyatt Technologies). Reversed-phase (RP)-HPLC analysis was performed on a Jupiter C4 column (Phenomenex) with TFA in water (0.1% w/v) for mobile phase A and TFA in acetonitrile (0.1% w/v) for mobile phase B. SDS-PAGE of the EPA protein was performed on a 4–20% Tris-glycine gel (Invitrogen) and stained with Coomassie blue as per the manufacturer's instructions. Amino-terminal sequencing was performed by the Research Technology Branch, NIAID, NIH using a Sequenator model Procise 494 HT (Applied Biosystems) as previously described [22,23]. Intact mass spectrometry was performed on an Agilent G6224A Accurate-Mass TOF with a dual ESI ion source and ion polarity in the positive mode. Protein was separated on a ZORBAX 300SB-C18 (Agilent) water + 0.05% TFA (solvent A) to acetonitrile + 0.05% TFA (solvent B) at a gradient of 0–70% B in 35 min. Acetic acid was added in a mixing tee placed before the electrospray inlet to the mass spectrometer at a ratio of 1:2 acetic acid to column eluent.

2.3. HCP content analysis

A quantitative slot blot assay was previously developed for determining the amount of *E. coli* HCPs in recombinantly expressed proteins [24] and was modified by using IRDye 800CW (LI-COR Biosciences) as the secondary antibody and measured with an Odyssey imaging instrument (LI-COR Biosciences) at 800 nm.

2.4. Peptide mapping and post-translational modifications (PTM)

Peptide mapping by LC-MS/MS analysis for composition of matter and PTMs was conducted using an Orbitrap Fusion Tribrid mass spectrometer (Thermo Electron) equipped with an EASY-Spray Ion Source and an Easy-nLC 1000. The EPA proteins were digested as follows. The protein was denatured at 0.1% RapiGest for 15 min at 80 °C. The protein was then reduced at 5 mM DTT and then alkylated at 15 mM iodoacetamide. Digestion was performed at a 1:40 trypsin:protein ratio overnight at 37 °C. Trifluoroacetic acid was used to quench the enzymatic reaction and degrade the RapiGest.

Liquid chromatography was carried out on a PepMap RSLC C18 column and a PepMap C18 Trap column operating at a 300 μL/min

flow rate with mobile phases A: 98% water + 2% acetonitrile + 0.1% formic acid and B: 98% acetonitrile + 2% water + 0.1% formic acid. The trypsin digest was diluted 1:20 in mobile phase A and 5 μL was injected. The MS/MS data were acquired during the gradient from 0% B to 40% B for 100 min, from 40% B to 80% B for 2 min and holding at 80% B for 2 min.

The mass spectrometer was operated in a data dependent acquisition mode with a cycle time of 3 s. First, the Orbitrap was used to acquire a high resolution full MS scan of all ions from m/z 400 to m/z 1800 at a resolution of 120,000 (m/z 190 at the target value of 4E5). The precursor ions are chosen with monoisotopic precursor selection, multiple charge states, and intensity threshold of 2.5E4. For the duration of 3 sec, most intense precursors were subjected to a fragmentation in the Ion Trap, where the precursor (the target value of 5E4) is isolated with the window of m/z 1, and activated using the activation q at 0.25 and CID collision energy at 35%, then MS2 spectra were detected with the Orbitrap at a resolution of 30,000 at m/z 190. Dynamic exclusion was enabled with the duration of 15 sec with ±10 ppm mass tolerance.

Mass spectrometry data was processed using a combination of proteomics tools with searches performed against a fasta file containing the recombinant EPA sequence and *Escherichia coli* BL21 (DE3) proteins deposited in the Uniprot KB (2/2018). Initial searches were performed on each acquisition with Preview, Byonic, and Byologic (ProteinMetrics) to help establish data and preparation quality, as well as, identify significant contributions from non-typical modifications. Follow-up analysis was performed using workflows implemented in Proteome Discoverer v2.2 (Thermo Scientific) with a subset of modifications based on matches within the ProteinMetrics workflow. A fixed carbamidomethylation (C) modification was utilized in combination with oxidation (M), deamination (N,Q), acetylation (K,S,T, N-term) carboxylation (K), amidation (Protein C-term), gluconylation/galactosyl (K, N-term), and phosphogluconylation (N-term), were all set as dynamic modifications for either their role as a sample handling-based modification or potential effect of bioactivity. Searches were performed using a Sequest HT search and modification site probabilities were calculated using PTMrs. Data was filtered at a 1% peptide FDR using protein profit as implemented within Proteome Discoverer. Area-under-the-curve based quantitation was used and missing peaks were found and quantified using an accurate mass and time tag approach. In instances where the algorithms either did perform the quantitation or quantified an aberrant peak manual validation was performed using a combination of MZmine2 (v2.32) and SeeMS (v3.0.6257) [25,26].

2.5. Mouse immunogenicity and assessment of antibody titers by ELISA

Mouse antisera were generated at the National Institutes of Health in compliance with guidelines of the National Institutes of Health Institutional Animal Care and Use Committee. In brief, groups of 5 BALB/c female mice were immunized by intramuscular injection with 1 μg of EPA purified following process A or B formulated on Alhydrogel® (Brenntag, Denmark) on days 0, 28 and exsanguinated on day 42. The reactivity of EPA specific antibodies was measured by ELISA using mouse antisera collected on days 0 and 42. Standard ELISA curves were prepared using 5-fold dilutions of mouse antisera. The ELISA plates were coated with 0.1 μg/mL of EPA (either from processes A or B). Goat anti-mouse, horseradish peroxidase-conjugated IgG (ThermoFisher Scientific) at 100 ng/well was used as secondary antibody, and 1-Step Ultra TMB-ELISA (Thermo Scientific) was used as developing solution, measuring the final absorbance at 450 nm. A reciprocal end-point titer at OD450 of 1 for each curve was determined by fitting the experimental points to a 4-parameters logistic function using the drc package for the statistical programming language R [27,28], and RStudio as an integrated development environment (IDE) software for R [29]. Mouse monoclonal antibody 7E3 was generated against EPA produced from process A following procedures as essentially described [30].

3. Results

3.1. Redevelopment of EPA purification

The redeveloped process modified the column chromatography steps following EPA binding and elution on a strong anion capture resin (Capto Q) (Fig. 1). Two mixed mode resins (MEP HyperCel™ and hydroxyapatite) were used in place of a traditional hydrophobic interaction resin (Phenyl Sepharose) with an additional strong anion resin (Q Sepharose) followed by size exclusion (Fig. 1). To effectively exploit the multimodal capabilities of the MEP resin [31,32], a combination of hydrophobic, ion exchange, and hydrogen bonding properties was used. First, we determined that 500 mM ammonium sulfate between pH 6.9 and 7.5 was needed to efficiently bind EPA. Next, we determined that once EPA bound the resin, the ammonium sulfate could be removed, and EPA would not elute at pH 6.2 which demonstrated that binding was not simply through a classical hydrophobic interaction mechanism. Lowering the pH to 4.0 to charge the MEP moiety, was necessary, but not enough, to elute EPA. This observation suggested that ion exchange is unlikely to be solely responsible for binding. Importantly, adding 1 M arginine in the wash buffer was critical for the release of many impurities at pH 4.7 and elution of EPA at pH 4.0. The hydroxyapatite sorbent was performed in a strictly pH driven application.

The revised chromatography process developed using mixed-mode resins enabled two process constraints to be overcome. First, the MEP column enabled marked enrichment of EPA while removing *E. coli* HCPs, endotoxin and product related impurities and then the CHT column allowed for the transition of the pH through the isoelectric point for subsequent elution of a soluble EPA. For the biochemical and biophysical studies comparing EPA from process A and process B, an in-house integrated scaled-down run was performed for each at quarter-scale relative to our cGMP manufacturing using feed stock from two 60 L working volume fermentations. The purified EPA from these different fermentation lots served as the EPA standards for processes A or B. The purification efficiencies for these one-quarter scale runs were 54% for Process A and 51% for Process B as quantitatively assessed by RP-HPLC (data not shown). The recovery efficiency of process B was also further improved by using a membrane cartridge for tangential flow filtration (TFF) in place of a hollow fiber cartridge for ultrafiltration prior to adsorption to the Capto Q resin. Altogether, the efficiency from fermentation harvest to final bulk during cGMP pilot-scale manufacturing at a contract manufacturing facility using process B was slightly better (70%) compared to earlier yields using process A (55–58% for three cGMP runs) as quantitatively assessed by RP-HPLC (data not shown).

3.2. Biophysical and biochemical analyses of EPA

The initial comparison of purified EPA derived from process A or B used a Coomassie blue stained SDS-PAGE gel (Fig. 2A) which showed a marked reduction of product related impurities under both reduced and non-reduced conditions as identified by in-gel digestion and mass spectroscopy (data not shown). We assessed the immunoreactivity of EPA using a mouse monoclonal antibody, identified as 7E3, and a polyclonal anti-exotoxin A serum. The immunoblotting profiles appeared similar for both forms of EPA using both reagents (Fig. 2B). Analytical SEC-MALS-HPLC showed

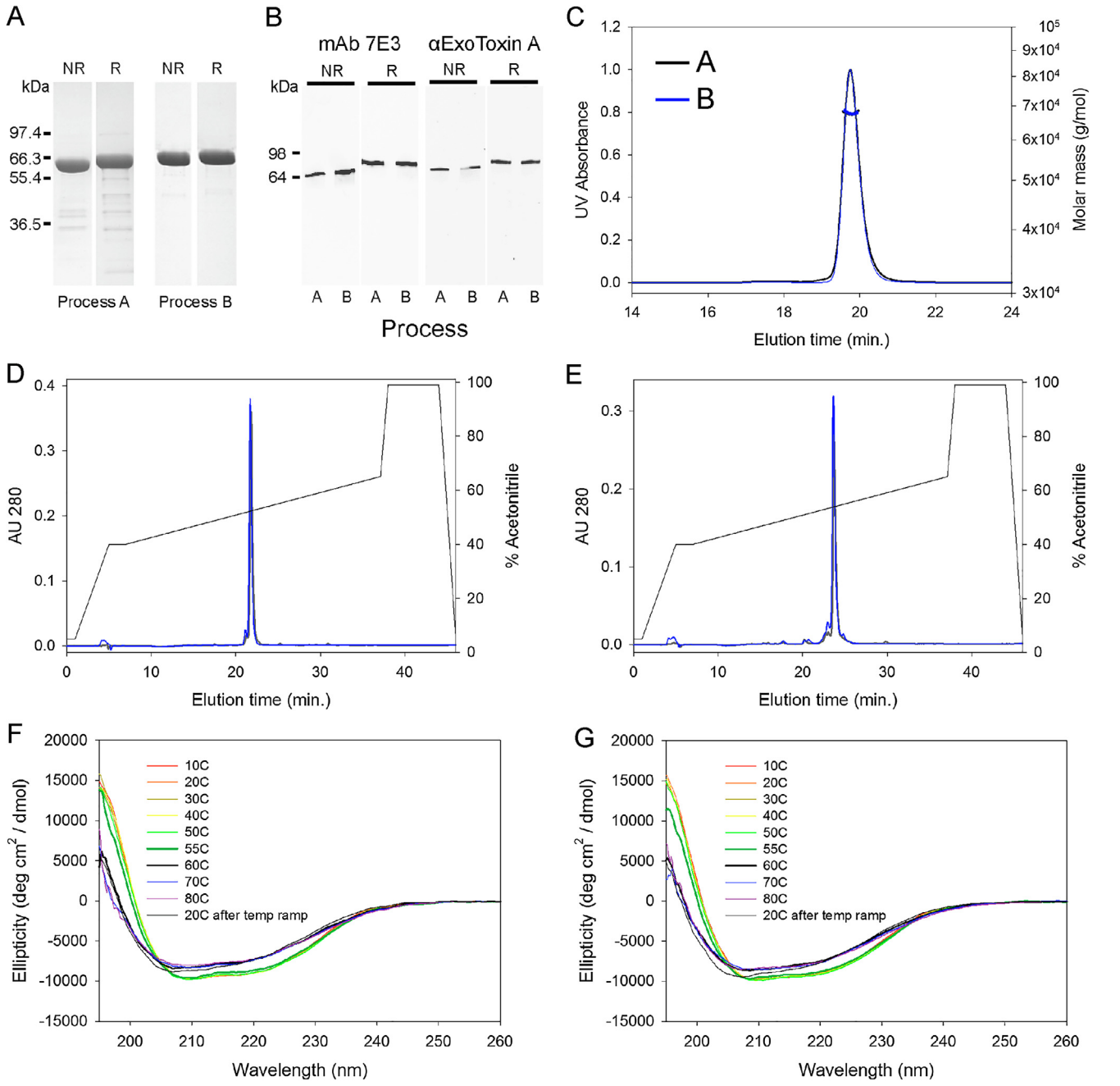

Fig. 2. Final bulk characterization of EPA derived from processes A or B. Panel A, Coomassie blue staining SDS-PAGE gel analysis. Panel B, immunoblot with EPA specific mAb 7E3 or polyclonal Exotoxin A under reducing (R) and non-reducing (NR) conditions. Panel C, SEC-MALS-HPLC analysis: EPA from process A, black line; process B, blue line. Panel D and E, RP-HPLC of non-reduced or reduced EPA from process A (black lines) or process B (blue lines), respectively. Panel F and G, FAR UV analysis of EPA from process A or B with heat denaturation at various temperatures. A marked change in the secondary structures of EPA are noted by the thickened blue and black lines at 55 °C and 60 °C. Negative controls for immunoblots are not shown.

similar chromatographic profiles (Fig. 2C), with a monomeric peak of 99.0% and 99.7% by process A and B, respectively. The molar masses were also comparable (67.7 kDa and 67.6 kDa, respectively) (Fig. 2C). Characterization of EPA from process A and B by RP-HPLC showed similar elution times and areas for the primary chromatographic peak under non-reduced (Fig. 2D) and reduced (Fig. 2E) conditions (93.1% versus 94.6% under non-reduced conditions, and 82.3% versus 81.0% under reduced conditions, respectively). An analysis of the secondary structures by FAR-UV showed that both forms of EPA had similar ellipticity curves when denatured by increasing temperature and that a major change in secondary structure was observed for both between 55 °C and 60 °C (Fig. 2F and G). Neither form of EPA appeared to completely refold following cooling to 20 °C (Fig. 2F and G). The identity of the purified material was also confirmed by intact mass spectrometry (66,977 Da and 66,978 Da, Process A and B respectively, compared to the expected mass of 66,975 Da) and N-terminal sequencing (ANLAEEAFDL).

3.3. Host cell protein content analysis

E. coli HCPs were quantitated using a platform specific immunoblot analysis which has a reported detection limit of 6.1 ng/mL using alkaline phosphatase as the substrate for detection of

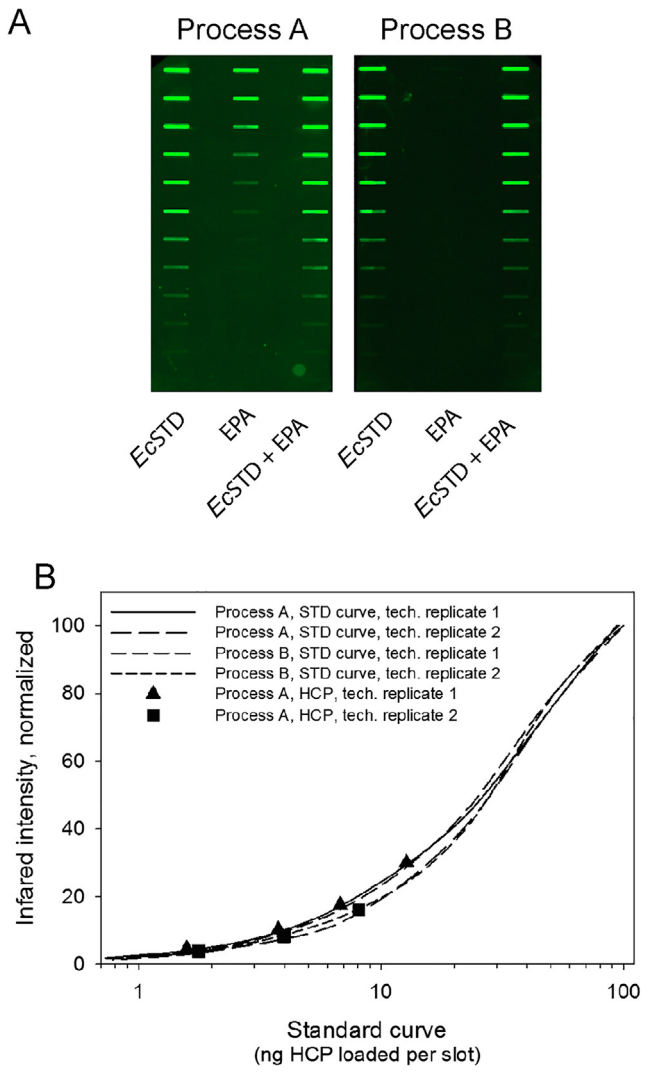

Fig. 3. *E. coli* HCP content analyses for EPA produced using process A or B. Panel A, HCP testing of EPA from process A (left panel) or process B (right panel). Lane identifiers for both upper panels are EPA, lane 1; *E. coli* (*Ec*) standard, lane 2; EPA + *Ec* standard mixed, lane 3. Panel B, graphical representation of the standard curves generated from panel A (solid and dashed lines representing technical replicates) and data points (▲ and ■) which represent independent HCP slot blot results observed in EPA from process A plotted within their respective standard curves.

antibody binding [24]. The detection limit was similar using IRDye 800CW secondary antibody (data not shown). The immunoblot method has unique qualities in that it may be used for both upstream and downstream HCP assessments [24]. A visual of the immunoblot results are shown in Fig. 3A along with a graphical representation of the standard curves and points on the curve for the HCP content identified in EPA from process A (Fig. 3B). The HCP content from process B was below the sensitivity of the test (Fig. 3A, right panel). The HCP content in the final bulk EPA from process A was 0.14% and 0.22% w/w (1419 and 2243 ppm) for the two replicates performed. The revised purification process B markedly reduced the HCP content in EPA to a level below the sensitivity of the assay.

3.4. Tryptic peptide analysis and post-translational modifications (PTMs)

Purified EPA derived from process A or B were peptide mapped by mass spectroscopy following trypsin digestion. The peptide coverage for both purification procedures used to produce EPA was greater than 99% (Fig. 4). A variance was noted in the amino acid sequence of recombinant EPA from the earliest report [12] that deleted E553 at which an amino acid substitution was noted at position V552 (or position V555 in Fig. 4 due to three additional non-native N-terminal amino acids that remained following cleavage of the *Salmonella typhimurium* outer membrane protein A signal peptide [13]) from leucine (L) to valine (V). The E553 amino acid deletion was expected in the pVC45Df+T expression plasmid [20] used in subcloning the *EPA* gene into the pET-24a(+) expression vector. The codon corresponding to L552 in the nucleotide sequences of both pET24a(+)/rEPA and pVC45Df+T plasmids had an unreported mutation from CTG to GTG which encoded for valine. The presence of valine was confirmed by evaluating the tryptic peptide fragments and mis-cleaved fragments of EPA. In all cases, the mass of the parent ion for the tryptic fragment containing V555 was within 1 ppm of the expected mass (see Supplementary Table S1) compared to an increase in mass of 14.0 Da if the amino acid at position V555 in Fig. 4 was leucine.

Supplementary data associated with this article can be found, in the online version, at https://doi.org/10.1016/j.vaccine.2018.09.037.

The EPA ionizing peptides were also compared for PTM (see Table 1 and Supplementary Table S1). As shown in Fig. 4 and Table 1, only a limited number of PTMs were observed; 89.3% of EPA peptides from process A and 89.8% of EPA peptides from process B had no PTMs. More importantly, only a limited number of PTMs were observed that appear to be similar for both regardless of the down-stream purification process. The most prominent PTM was deamidation, which were likely induced by the trypsin digestion [33]. Amidation was searched as a C-terminal modification [34] and was present on K615, with slightly more for process A at an average of 4.0% of total peptides. Acetylation was seen at several locations but occurred at 100% for Q356. Gluconoylation, a common posttranslational glycation observed in the fermentation of *E. coli* cells that can adversely affect the quality of recombinant protein [35], was observed at several sites, but never above 2% of the total peptides. Carboxylation and phosphogluconylation were not observed in any of the samples.

3.5. Immunogenicity of EPA in mice

Pooled serum from groups of BALB/c mice immunized with EPA produced from process A or B formulated on Alhydrogel® yielded similar reciprocal ELISA titers at an OD1 independent of the plate antigen (3.40E6 VS 3.77E6 on EPA from process A or 1.76E6 vs 2.12E6 on EPA from process B).

4. Discussion

Chemical conjugation of EPA to polysaccharides and weakly immunogenic proteins has been used to produce effective immunogens [9,11,16,36]. In malaria vaccine development of transmission blocking vaccines chemical conjugation to EPA has been critical for demonstrating improved immunogenicity while maintaining safety [11]. A trial in the U.S.A. was the first demonstration of biological activity of a *P. falciparum* malaria transmission blocking vaccine formulated on Alhydrogel™ in humans [11] and more recently, similar observations were obtained in a phase 1 trial in Mali (manuscript in preparation, clinical trials.gov NCT02334462).

In the original purification process, the quality attributes for EPA were within the acceptance criteria for cGMP pilot-scale production with the exception for the HCP content. Possibly due to scale-up, the HCP concentration was consistently near the threshold for an out-of-specification determination. The search for alternative resins

Fig. 4. Primary amino acid sequence of EPA and tryptic peptide coverage map for EPA produced following processes A or B, and identification of post-translational modifications (PTM) by LC/MS/MS. Bold text indicates peptides not identified in tryptic peptide mapping. Specific PTMs observed in both technical replicates at >1% intensity are noted by the colored highlighted letter(s) (gray for gluconylation, yellow for acetylation and green for amidation) and italics designates N-terminal modifications.

Table 1
Post-translational modifications observed for specific amino acids (AA) within EPA derived from process A or B.

PTM[#]		Acetylation				Amidation				Gluconylation			
Location	AA	A1	A2	B1	B2	A1	A2	B1	B2	A1	A2	B1	B2
1	A	–	–	–	–	–	–	–	–	0.58%	0.56%	1.74%	1.98%
23	K	–	–	–	–	–	–	–	–	0.01%	0.01%	0.02%	0.03%
40	T	0.09%	**	0.10%	0.13%	–	–	–	–	–	–	–	–
158	A	0.43%	*	0.64%	0.48%	–	–	–	–	–	–	–	–
167	T	0.43%	0.80%	0.08%	0.04%	–	–	–	–	–	–	–	–
176	S	0.50%	0.49%	**	–	–	–	–	–	–	–	–	–
243	K	–	–	–	–	–	–	–	–	0.01%	0.01%	0.30%	0.38%
356	Q	**	**	100%	**	–	–	–	–	–	–	–	–
608	K	–	–	–	–	–	–	–	–	0.10%	0.09%	0.33%	0.35%
615	K	–	–	–	–	3.95%	4.10%	1.39%	0.53%	–	–	–	–

[#] Technical replicates are included for each sample from process A or B.
[*] xxx.
[**] xxx.

identified MEP resin which is a multimodal chromatography matrix that can be used to capture target protein from untreated feedstocks showing its value as a purification media [32]. In general, at high-levels of salt typical for HIC, binding is effective and target protein can be recovered by desalting, lowering the pH, or a combination of the two. Below pH 4.8, the ionizable MEP resin is protonated allowing for charge displacement or pH dependent elution [32]. In the case of EPA, binding was dependent on the salt levels and it was necessary to add 500 mM ammonium sulfate in the feedstock to adsorb EPA. Once EPA bound the resin, the ammonium sulfate could be removed, and EPA remained bound thereby strongly suggesting that binding was not through a classical HIC mechanism. Lowering the pH to 4.0 was necessary but not sufficient to elute product suggesting desorption by ionic repulsion was not solely responsible. Importantly, adding 1 M arginine in the wash buffer was critical for the release of most of the non-product related impurities at pH 5.0 and subsequent elution of EPA at pH 4.0, possibly implicating a hydrogen bonding effect [31].

The theoretical isoelectric point of EPA is 5.3 and when attempting to buffer exchange EPA using ultrafiltration from the MEP

eluent (at pH 4.0) into a neutral pH buffer for further processing, a sizable portion of the EPA would aggregate (data not shown). Binding of EPA from the MEP eluent to a CHT resin at pH 6.0 and elution at pH 7.5 served two purposes, product was buffer exchanged without precipitation and additional HCPs of a different molecular weight than EPA were removed (data not shown).

An important aim of this study was to establish the biophysical and biochemical comparability of the two purified forms of EPA derived from process A or B were highly similar. To this end, the full-biochemical and biophysical characterization demonstrated that the identity, purity, solubility as well as secondary structure appeared highly similar, including their evaluation by RP-HPLC and analytical SEC-MALS-HPLC. Furthermore, we demonstrated that the EPA specific mAb 7E3 is suitable for recombinant protein characterization by immunoblot. The most extensive demonstration of the comparability of EPA derived from processes A and B was the tryptic peptide mapping studies and PTM analysis. Of note, 99% of the protein was identified in the peptide mapping and more than 90% of the tryptic peptide fragments were accounted for as non-modified peptides. Of the 10% of the peptides identified with PTMs (amidation, deamidation or acetylation), the majority were potentially derived from tryptic digestion and process handling [33]. We also screened for ADP-ribosylation, gluconylation, phosphogluconylation, and sulfation, but there was no indication of their respective modifications. Finally, we noted that the expected native leucine at position 552 (or position 555 in Fig. 4) had at some point been substituted with the conserved amino acid, valine. Given that plasmid pVC45Df+T contained the nucleotide sequence GTG at codon 552 which encodes for valine and not CAG encoding for glutamic acid, it seems that this point mutation occurred when the E553 deletion was introduced ([12,20] and D. Fitzgerald and I. Pastan, personal communication).

The HCP content in clinical material is an important consideration during development [37]. Bulk EPA with the levels of *E. coli* HCP approaching the acceptance criteria required reprocessing, prior to conjugation, which resulted in both time and material losses. With respect to EPA used in clinical trials, the HCP content was less than 0.1% w/w EPA following reprocessing. The addition of MEP and CHT column chromatography steps resulted in product with highly similar biophysical and biochemical properties based on extensive characterization (Figs. 2–4) but with a markedly improved HCP content using a process/platform specific immunoblot assay [24]. The HCP levels of the one-quarter EPA standard from process A averaged 0.18% w/w HCP and for other research lots ranged up to 0.8% w/w HCP. The minimum detectable level by the immunoblot assay is 0.0012% w/w HCP. Multiple lots from process B were below this level of sensitivity which represented at least a hundred-fold reduction in the HCP level. A similar reduction in the abundance of HCPs was observed when comparing processes, A and B by quantitative mass spectroscopy (manuscript in preparation).

The process changes reported here have yielded an EPA with highly similar quality characteristics and immunogenicity as the original EPA process which had already been used in multiple clinical trials [11] (and NCT02334462 and NCT02942277) but with more robust removal of *E. coli* HCP. With a reduced HCP content, the safety profiles of future conjugated malaria vaccines are likely to be unchanged. Considering the number of clinical trials that have used EPA as a carrier from various sources and demonstrated safety, EPA is likely a suitable carrier for use in human vaccines.

Conflict of interest

The authors declare no competing interests.

Acknowledgements

We appreciate the technical assistance for formulating EPA by Kelly Rausch, and Emma Barnafo, and performance of the small animal immunizations by Brandi Butler, and Lynn Lambert. Weili Dai provided technical support for performance of HCP assays. We also thank Drs. Duck-Yeon Lee, Glenn Nardone, and Brian Martin from RTB for support in the biophysical characterization of EPA. Finally, we appreciated Drs. David Fitzgerald and Ira Pastan for their assistance in the clarification of the unreported mutation in EPA. This work was supported by the Intramural Research Program of the National Institute for Allergy and Infectious Diseases, National Institutes of Health.

References

[1] Avery OT, Goebel WF, Babers FH. Chemo-immunological studies on conjugated carbohydrate-proteins: VII. Immunological specificity of antigens prepared by combining alpha- and beta-glucosides of glucose with proteins. J Exp Med 1932;55(5):769–80.
[2] Schneerson R, Robbins JB, Parke Jr JC, Bell C, Schlesselman JJ, Sutton A, et al. Quantitative and qualitative analyses of serum antibodies elicited in adults by *Haemophilus influenzae* type b and pneumococcus type 6A capsular polysaccharide-tetanus toxoid conjugates. Infect Immun 1986;52(2):519–28.
[3] Wenger JD, Pierce R, Deaver KA, Plikaytis BD, Facklam RR, Broome CV. Efficacy of *Haemophilus influenzae* type b polysaccharide-diphtheria toxoid conjugate vaccine in US children aged 18-59 months. Haemophilus Influenzae Vaccine Efficacy Study Group. Lancet 1991;338(8764):395–8.
[4] Tregnaghi MW, Saez-Llorens X, Lopez P, Abate H, Smith E, Posleman A, et al. Efficacy of pneumococcal nontypable *Haemophilus influenzae* protein D conjugate vaccine (PHiD-CV) in young Latin American children: a double-blind randomized controlled trial. PLoS Med 2014;11(6):e1001657.
[5] Fu J, Bailey FJ, King JJ, Parker CB, Robinett RS, Kolodin DG, et al. Recent advances in the large scale fermentation of *Neisseria meningitidis* group B for the production of an outer membrane protein complex. Biotechnology (N Y) 1995;13(2):170–4.
[6] Donnelly JJ, Deck RR, Liu MA. Immunogenicity of a *Haemophilus influenzae* polysaccharide-*Neisseria meningitidis* outer membrane protein complex conjugate vaccine. J Immunol 1990;145(9):3071–9.
[7] Masforrol Y, Gil J, Garcia D, Noda J, Ramos Y, Betancourt L, et al. A deeper mining on the protein composition of VA-MENGOC-BC(R): an OMV-based vaccine against *N. meningitidis* serogroup B and C. Hum Vaccines Immunother 2017;13(11):2548–60.
[8] Zuercher AW, Horn MP, Que JU, Ruedeberg A, Schoeni MH, Schaad UB, et al. Antibody responses induced by long-term vaccination with an octovalent conjugate *Pseudomonas aeruginosa* vaccine in children with cystic fibrosis. FEMS Immunol Med Microbiol 2006;47(2):302–8.
[9] Hoogsteder PH, Kotz D, van Spiegel PI, Viechtbauer W, van Schayck OC. Efficacy of the nicotine vaccine 3′-AmNic-rEPA (NicVAX) co-administered with varenicline and counselling for smoking cessation: a randomized placebo-controlled trial. Addiction 2014;109(8):1252–9.
[10] Thiem VD, Lin FY, Canh DG, Son NH, Anh DD, Mao ND, et al. The Vi conjugate typhoid vaccine is safe, elicits protective levels of IgG anti-Vi, and is compatible with routine infant vaccines. Clin Vaccine Immunol: CVI 2011;18(5):730–5.
[11] Talaat KR, Ellis RD, Hurd J, Hentrich A, Gabriel E, Hynes NA, et al. Safety and immunogenicity of Pfs25-EPA/Alhydrogel(R), a transmission blocking vaccine against *Plasmodium falciparum*: an open label study in malaria naive adults. PLoS ONE 2016;11(10):e0163144.
[12] Lukac M, Pier GB, Collier RJ. Toxoid of *Pseudomonas aeruginosa* exotoxin A generated by deletion of an active-site residue. Infect Immun 1988;56(12):3095–8.
[13] Qian F, Wu Y, Muratova O, Zhou H, Dobrescu G, Duggan P, et al. Conjugating recombinant proteins to *Pseudomonas aeruginosa* ExoProtein A: a strategy for enhancing immunogenicity of malaria vaccine candidates. Vaccine 2007;25(20):3923–33.
[14] Radtke AJ, Anderson CF, Riteau N, Rausch K, Scaria P, Kelnhofer ER, et al. Adjuvant and carrier protein-dependent T-cell priming promotes a robust antibody response against the *Plasmodium falciparum* Pfs25 vaccine candidate. Sci Rep 2017;16(7):40312.
[15] Qian F, Reiter K, Zhang Y, Shimp Jr RL, Nguyen V, Aebig JA, et al. Immunogenicity of self-associated aggregates and chemically cross-linked conjugates of the 42 kDa *Plasmodium falciparum* merozoite surface protein-1. PLoS ONE 2012;7(6):e36996.
[16] Jones DS, Rowe CG, Chen B, Reiter K, Rausch KM, Narum DL, et al. A method for producing protein nanoparticles with applications in vaccines. PLoS ONE 2016;11(3):e0138761.
[17] Shimp Jr RL, Rowe C, Reiter K, Chen B, Nguyen V, Aebig J, et al. Development of a Pfs25-EPA malaria transmission blocking vaccine as a chemically conjugated nanoparticle. Vaccine 2013;31(28):2954–62.

[18] Kaslow DC, Biernaux S. RTS,S: toward a first landmark on the Malaria Vaccine Technology Roadmap. Vaccine 2015;33(52):7425–32.
[19] Rts SCTP. Efficacy and safety of RTS, S/AS01 malaria vaccine with or without a booster dose in infants and children in Africa: final results of a phase 3, individually randomised, controlled trial. Lancet 2015;386(9988):31–45.
[20] Fattom A, Shiloach J, Bryla D, Fitzgerald D, Pastan I, Karakawa WW, et al. Comparative immunogenicity of conjugates composed of the *Staphylococcus aureus* type 8 capsular polysaccharide bound to carrier proteins by adipic acid dihydrazide or N-succinimidyl-3-(2-pyridyldithio)propionate. Infect Immun 1992;60(2):584–9.
[21] Fass R, van de Walle M, Shiloach A, Joslyn A, Kaufman J, Shiloach J. Use of high density cultures of *Escherichia coli* for high level production of recombinant *Pseudomonas aeruginosa* exotoxin A. Appl Microbiol Biotechnol 1991;36 (1):65–9.
[22] Uchime O, Herrera R, Reiter K, Kotova S, Shimp Jr RL, Miura K, et al. Analysis of the conformation and function of the *Plasmodium falciparum* merozoite proteins MTRAP and PTRAMP. Eukaryot Cell 2012;11(5):615–25.
[23] Zhu D, Wu Y, McClellan H, Dai W, Rausch K, Jones D, et al. Accelerated and long term stability study of Pfs25-EPA conjugates adjuvanted with Alhydrogel(R). Vaccine 2017;35(24):3232–8.
[24] Zhu D, Saul AJ, Miles AP. A quantitative slot blot assay for host cell protein impurities in recombinant proteins expressed in *E. coli*. J Immunol Methods 2005;306(1–2):40–50.
[25] Pluskal T, Castillo S, Villar-Briones A, Oresic M. MZmine 2: modular framework for processing, visualizing, and analyzing mass spectrometry-based molecular profile data. BMC Bioinf 2010;23(11):395.
[26] Chambers MC, Maclean B, Burke R, Amodei D, Ruderman DL, Neumann S, et al. A cross-platform toolkit for mass spectrometry and proteomics. Nat Biotechnol 2012;30(10):918–20.
[27] Ritz C, Baty F, Streibig JC, Gerhard D. Dose-response analysis using R. PLoS ONE 2015;10(12):e0146021.
[28] Team RC. A language and environment for statistical computing. R Foundation for Statistical Computing. Vienna, Austria; 2017.
[29] Team RS. RStudio: Integrated Development for R. RStudio, Inc Boston, MA; 2015.
[30] Narum DL, Ogun SA, Thomas AW, Holder AA. Immunization with parasite-derived apical membrane antigen 1 or passive immunization with a specific monoclonal antibody protects BALB/c mice against lethal *Plasmodium yoelii yoelii* YM blood-stage infection. Infect Immun 2000;68(5):2899–906.
[31] Lin DQ, Tong HF, Wang HY, Shao S, Yao SJ. Molecular mechanism of hydrophobic charge-induction chromatography: interactions between the immobilized 4-mercaptoethyl-pyridine ligand and IgG. J Chromatogr A 2012;19(1260):143–53.
[32] Burton SC, Harding DR. Hydrophobic charge induction chromatography: salt independent protein adsorption and facile elution with aqueous buffers. J Chromatogr A 1998;814(1–2):71–81.
[33] Li X, Cournoyer JJ, Lin C, O'Connor PB. Use of 18O labels to monitor deamidation during protein and peptide sample processing. J Am Soc Mass Spectrom 2008;19(6):855–64.
[34] Suckau D, Resemann A. T3-sequencing: targeted characterization of the N- and C-termini of undigested proteins by mass spectrometry. Anal Chem 2003;75 (21):5817–24.
[35] Aon JC, Caimi RJ, Taylor AH, Lu Q, Oluboyede F, Dally J, et al. Suppressing posttranslational gluconoylation of heterologous proteins by metabolic engineering of *Escherichia coli*. Appl Environ Microbiol 2008;74(4):950–8.
[36] Szu SC, Hunt S, Xie G, Robbins JB, Schneerson R, Gupta RK, et al. A human IgG anti-Vi reference for *Salmonella typhi* with weight-based antibody units assigned. Vaccine 2013;31(15):1970–4.
[37] Le Merdy S. Selection of clarification methods for improved downstream performance and economics. Bioprocess J 2015;14(3):50–3.